The LINNEAN SOCIETY of London BIOLOGICAL Journal of the Linnean Society

Biological Journal of the Linnean Society, 2014, **111**, 375–390. With 7 figures

Association between integration structure and functional evolution in the opercular four-bar apparatus of the threespine stickleback, *Gasterosteus aculeatus* (Pisces: Gasterosteidae)

HEATHER A. JAMNICZKY[1]*, EMILY E. HARPER[2], REBECCA GARNER[2], WILLIAM A. CRESKO[3], PETER C. WAINWRIGHT[4], BENEDIKT HALLGRÍMSSON[5]* and CHARLES B. KIMMEL[2]*

[1]*Department of Cell Biology & Anatomy and McCaig Institute for Bone and Joint Health, Faculty of Medicine, University of Calgary, 3280 Hospital Drive NW, Calgary, AB T2N 3Z6, Canada*
[2]*Institute of Neuroscience, University of Oregon, 222 Huestis Hall, Eugene, OR 97403, USA*
[3]*Institute of Ecology and Evolution, University of Oregon, 312 Pacific Hall, Eugene, OR 97403, USA*
[4]*Department of Evolution & Ecology, University of California Davis, 1 Shields Avenue, Davis, CA 95616, USA*
[5]*Department of Cell Biology & Anatomy, McCaig Institute for Bone and Joint Health, and Alberta Children's Hospital Research Institute, Faculty of Medicine, University of Calgary, 3280 Hospital Drive NW, Calgary, AB T2N 3Z6, Canada*

Received 29 July 2013; revised 11 September 2013; accepted for publication 11 September 2013

Phenotypes may evolve to become integrated in response to functional demands. Once evolved, integrated phenotypes, often modular, can also influence the trajectory of subsequent responses to selection. Clearly, connecting modularity and functionally adaptive evolution has been challenging. The teleost skull and jaw structures are useful for understanding this connection because of the key roles that these structures play in feeding in novel environments with different prey resources. In the present study, we examined such a structure in the threespine stickleback: the opercular four-bar lever that functions in jaw opening. Comparing oceanic and two fresh-water populations, we find marked phenotypic divergence in the skull opercular region, and the major axes of morphological and functional variation of the lever are found to be highly correlated. All three populations share the same global skull integration structure, and a conserved, strongly-supported modular organization is evident in the region encompassing the lever. Importantly, a boundary between two modules that subdivides the lever apparatus corresponds to the region of most prominent morphological evolution. The matched modular phenotypic and functional architecture of head and jaw structures of stickleback therefore may be important for facilitating their rapid adaptive transitions between highly divergent habitats. © 2013 The Linnean Society of London, *Biological Journal of the Linnean Society*, 2014, **111**, 375–390.

ADDITIONAL KEYWORDS: evolutionary developmental biology – modularity – opercular four-bar lever – phenotypic evolution – sticklebacks.

INTRODUCTION

The relationship between phenotypic correlations and evolutionary change was first suggested by Darwin (1859), and subsequently developed into an hypothesis that morphological covariances evolve to facilitate the functional integration of complex suites of traits (Olson & Miller, 1958). Investigating the complex relationship between developmental genetic architectures and phenotypic covariances has become a major thrust of evolutionary developmental biology (Thompson, 1917; Lande, 1979; Cheverud, 1982; Zelditch, 1988; Hallgrimsson *et al.*, 2007a; Jamniczky

*Corresponding author. E-mail: hajamnic@ucalgary.ca; bhallgri@ucalgary.ca; kimmel@uoneuro.uoregon.edu

& Hallgrimsson, 2009). A prediction from theory is that functional integration will often be manifested in modular phenotypic and developmental covariances, in which traits within a module covary more tightly with one another than they do with traits in other modules (Olson & Miller, 1958; Cheverud, 1982; Wagner & Altenberg, 1996; Klingenberg, 2008).

Phenotypic covariance and modularity result from the structuring of variation by developmental processes (Hendrikse, Parsons & Hallgrimsson, 2007; Hallgrimsson *et al*., 2009). These developmental processes are the products of evolution and can thus be influenced by natural selection. Because functionally important aspects of phenotypes are often composites of several morphological structures, selection will tend to produce correlations among functionally-related traits by acting on underlying developmental architecture (Cheverud, 1996a). However, development can also constrain or bias evolutionary change through the tendency to produce functional integration (Raff, 1996; Wagner, Booth & Bagheri, 1997; Klingenberg *et al*., 2012). Once established, correlations among functionally-related traits enhance the evolvability of complex developmental systems because development will tend to produce a functionally coordinated response to selection (Wagner & Altenberg, 1996; Hansen & Houle, 2008).

Phenotypic and developmental modules are variously thought of as discrete and non-overlapping (Raff, 1996; Wagner *et al*., 1997) or as complex and overlapping (Hallgrimsson *et al*., 2007b; 2009). The latter view is based on the idea that multiple developmental processes acting at different times in development produce overlapping influences on the phenotypic covariation structure in complex morphologies. This 'palimpsest hypothesis' (Hallgrimsson *et al*., 2009) holds that covariance structures are often the result of multiple developmental influences that overlap in time and space and can partially 'overwrite' each other. Changes in the relative variances of covariance-generating processes can produce alterations in phenotypic covariation structure without altering the developmental interactions that enable covariation to appear. In this view, covariance structures may be more developmentally labile and less likely to bias or constrain evolutionary change than they first appear (Jamniczky & Hallgrimsson, 2009; Sanger *et al*., 2011).

Disentangling this complex relationship between developmental architecture and natural selection in producing functionally integrated modules is difficult because the direction of causality can be hard to establish (Wagner, 1990; Cheverud, 1996a; Jones, Arnold & Bürger, 2007; Jamniczky & Hallgrimsson, 2009, 2011; Sanger *et al*., 2011). A useful approach is to study functionally important traits that have evolved in parallel in different lineages adapted to distinct environments. Several hypotheses can be presented for the relationship of phenotypic modularity with parallel evolutionary change. First, the complex traits may not exhibit any modularity, and could therefore completely explore phenotype space during evolution. Alternatively, modular phenotypic architecture may have evolved and now structures phenotypic changes, although remaining constant in the different lineages. Under this hypothesis, evolution of a complex phenotype occurs through coordinated changes within modules that are free to evolve independently of one another. Finally, the modular architecture itself might evolve to be different between the distinct environments. These hypotheses can be labelled 'modular absence', 'modular stasis' and 'modular reorganization', respectively.

In the present study, we take advantage of a natural experiment to test hypotheses of modular evolution by comparing two separate lacustrine populations of threespine stickleback (*Gasterosteus aculeatus*) with an oceanic population that diverged from a common ancestral population, approximately 10 000 years ago (Hohenlohe *et al*., 2010). The ability to combine assessment of modularity and function in a well characterized model organism within a unique ecological and evolutionary setting offers a novel opportunity to better understand the relationship between genetic architecture and phenotypic modularity with respect to shaping microevolutionary trajectories.

Decades of ecological research on stickleback have documented variation in body shape and head and jaw structures that is correlated with different habitats (McPhail, 1993; Walker, 1997; Schluter *et al*., 2010; Willacker *et al*., 2010; Aguirre & Bell, 2012). For example, oceanic sticklebacks have been found to feed on planktonic prey using gut content analysis and stable isotope analyses, which is a foraging ecology that is maintained in so-called 'limnetic' freshwater populations of stickleback existing in large, oligotrophic lakes (McPhail, 1984; Kassen, Schluter & McPhail, 1995). Consequently, both oceanic and limnetic stickleback have more fusiform body shapes that facilitate the exploitation of patchily dispersed planktonic resources (Lavin & McPhail, 1986, 1987; Cresko & Baker, 1996; Walker & Bell, 2000). By contrast, a majority of freshwater populations of stickleback, including those examined in the present study, exist in small, shallow lakes, and have evolved a divergent 'benthic' morphology that allows the efficient utilization of larger, more evenly distributed benthic macroinvertebrates (Lavin & McPhail, 1985, 1986, 1987; Walker & Bell, 2000).

An additional advantage is that sticklebacks are an increasingly prominent subject of study in evolutionary developmental biology (Bell & Foster, 1994;

Cresko *et al*., 2004; Schluter *et al*., 2010; Kimmel *et al*., 2012), for which novel genomic resources (Kingsley *et al*., 2004; Hohenlohe *et al*., 2010), including multiple stickleback genome sequences (Jones *et al*., 2012), are available.

Promising foci of modularity research are head and jaw structures, including skull lever systems that function in jaw movement, as a result of the prominent role these structures play in acquiring resources in animals (Atchley & Hall, 1991; Albertson *et al*., 2005; Goswami, 2006; Tokita, Kiyoshi & Armstrong, 2007; Zelditch *et al*., 2008; Fish *et al*., 2011; Sanger *et al*., 2011; Parnell, Hulsey & Streelman, 2012). Functional morphological studies in fishes, including the stickleback, have been particularly informative because of the distinct food types found in different habitats that require different phenotypic adaptations (Anker, 1974; Liem, 1974; Westneat, 1990; Wainwright *et al*., 2004; Hulsey, Fraser & Streelman, 2005; Wainwright, 2007; Parsons, Márquez & Albertson, 2012). Focusing on a set of four opercular bones that neighbour one another in the hyoid arch, we are able to compare evolutionary changes (or a lack thereof) in both form and covariation structure with alterations in how the set functions in feeding mechanics. We have previously shown that the shape of one of these bones (i.e. the opercle) has evolved rapidly and in parallel in geographically diverse freshwater stickleback populations (Kimmel *et al*., 2005; 2008, 2012). Functioning with the other three opercular bones, the subopercle, preopercle and interopercle, the opercle is the central component of a mechanical linkage system within the head skeleton of many or all teleosts, namely the opercular four-bar lever, which plays an important role in jaw opening and feeding (Anker, 1974; Muller, 1996). Through this lever system, a posterior–dorsal rotation of the opercle, via the opercular levator muscle, is translated into a ventral rotation of the lower jaw about the articular–quadrate joint. Shape change of the opercle, comprising the major portion of one of the lever arms, is expected to importantly affect the mechanical efficiency of the four-bar lever.

A second jaw-opening linkage is also present in the same region: the hyoid–mandibular system (Liem, 1970; Lauder, 1985). Here, contraction of the sternohyoid muscle causes a posterior rocking of the proximal end of the ceratohyal, placing tension on a ligament that connects the posterior end of the ceratohyal to the interopercle. Through the interopercle, the tension causes jaw depression in the same way as by the opercular four-bar lever. Hence, evolvability of the interopercle might be expected to be of particular interest because two separate functional systems funnel through the same bone in jaw opening.

Although both the opercular four-bar lever and the hyoid–mandibular system mechanically contribute to jaw depression, it is widely accepted that the hyoid–mandibular system is dominant during suction feeding movements (Anker, 1974; Westneat, 1990; de Visser & Barel, 1998; Van Wassenbergh *et al*., 2005). Nevertheless, disruption of the opercular four-bar system has been shown to substantially alter prey capture kinematics, resulting in a 70% reduction in lower jaw rotation in blackchin tilapia (Durie & Turingan, 2004). The opercular four-bar lever is thus one linkage in a complex musculoskeletal system that mediates jaw depression in teleosts. It contributes to lower jaw movements that take place during prey capture and respiration (Anker, 1985).

Here, we first investigate the nature of the morphological change in the region encompassing the four opercular bones and the hyoid–mandibular system, and its association with feeding mechanics. We predict that adaptation for foraging in alternative oceanic and freshwater environments has produced a modular organization of these morphological characters. We then ask whether skull modularity could influence adaptive divergence between environments through either 'modular stasis' or 'modular reorganization' hypotheses. We predict that, if modularity is observed to be stable among the oceanic and freshwater populations, then prominent evolution might occur between modules, and not within or across them. Alternatively, modularity might itself evolve, in which case modular reorganization might be expected to parallel changes in skull shape. To test these hypotheses, we compare the skull phenotypes of laboratory-reared, single-pair families derived from three previously studied Alaskan stickleback populations, including putatively ancestral oceanic fish from Rabbit Slough and freshwater populations from two nearby lakes (Boot Lake and Bear Paw Lake) that likely have independently evolved from oceanic ancestors (Cresko *et al*., 2004; Hohenlohe *et al*., 2010; 2012).

MATERIAL AND METHODS

Sample composition

Threespine stickleback were originally obtained from wild Alaskan populations, which were used to create stable lines in the laboratory. These populations included an anadromous population from Rabbit Slough [$N = 29$ (skull); 22 (four opercular bone set)] and two lacustrine populations from Boot Lake [$N = 31$ (skull); 25 (four opercular bone set)] and Bear Paw Lake [$N = 32$ (skull); 18 (four opercular bone set)]. The fish in the present study, used in previous studies of opercle shape (Kimmel *et al*., 2008, 2012) were obtained from single-pair crosses and were laboratory reared for five generations in a consistent

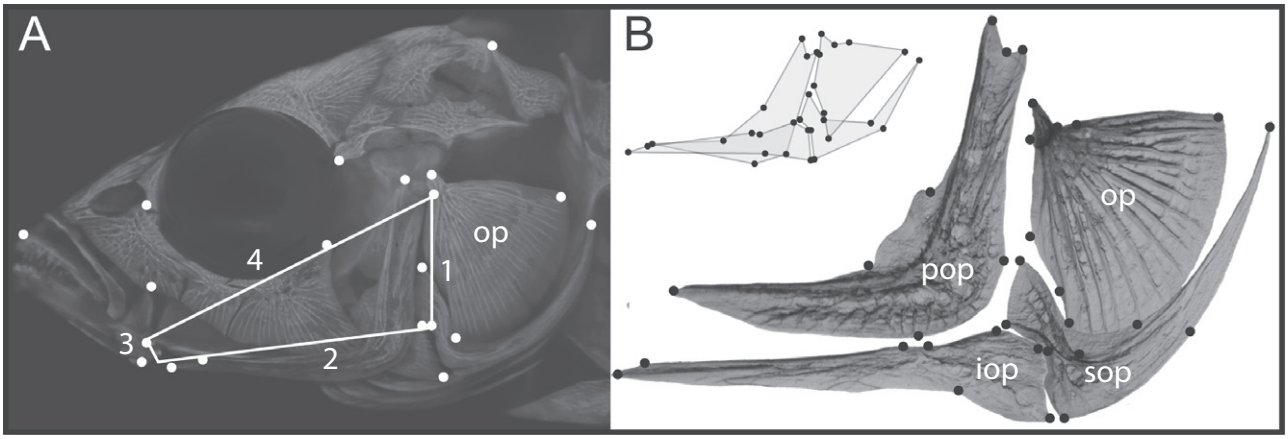

Figure 1. Two-dimensional landmark configurations for the whole skull (A) and the four opercular bones representing three links of the opercular four-bar lever (B), collected from three populations of threespine stickleback (*Gasterosteus aculeatus*). The white polygon in (A) indicates the approximate location of the opercular four-bar lever, with links numbered as follows: opercular = 1; ventral = 2; jaw = 3; fixed = 4. The inset in (B) indicates the correct anatomical relationships between the four opercular bones, which have been disarticulated for landmarking (for details, see text and Fig. 2). IOP, interopercle; OP, opercle; POP, preopercle; sop, subopercle.

controlled environment to eliminate environmental effects on phenotypic variation. After reaching a standard length of 28–30 mm (juvenile stage: Rabbit Slough = 100 days postfertilization, Boot Lake = 96 days postfertilization, Bear Paw Lake = 76 days postfertilization), fish were fixed in 4% paraformaldehyde, stained with 0.025% alizarin red and stored in 50% isopropanol.

Photography, landmarking, and biomechanical assessment

Two sets of landmark data were assembled to fully assess shape and function in the opercular four-bar lever and its component bones. An initial set of landmarks was digitized at key locations on photographs of side views of the alizarin red stained skulls to show both the overall skull shapes and the dimensions of the four-bar lever arms (Figs 1A, 2A). A Procrustes superimposition was applied to these skull shape landmarks to remove information related to rotation, transformation, and scaling, and these superimposed data were used for further analysis of skull shape. The landmarks delimiting the four-bar lever were used for biomechanical assessment of this structure. Opercular four-bar lever link lengths, including the opercular, ventral, jaw, and fixed links, were computed from the whole skull landmark set (Fig. 2A) and are as follows: opercular link = the distance between landmark 9 and the mean position between landmarks 10 and 11; ventral link = the distance between the mean position between landmarks 10 and 11 to the mean position between landmarks 4 and 12; jaw link = the distance between the mean position between landmarks 4 and 12 to landmark 13; fixed link = the distance between landmark 13 and landmark 9. We measured the starting position of the four-bar lever as the diagonal distance between landmarks 13 and the mean of 10 and 11. The four-bar lever transmission coefficient (K_T) was calculated as the output per input ratio of degrees of output rotation in the lower jaw link, which was solved geometrically based on 5° of input rotation in the opercle (Westneat, 1990). Four-bar linkages possess one degree of freedom, allowing all angles to be calculated from a known change in the input angle. K_T was calculated separately for each of the 92 individuals in the study.

Following the collection of landmark and biomechanical data for complete skulls, the four opercular bones (opercle, subopercle, interopercle, preopercle) were dissected out and landmarked individually to include points not present on the surface of the articulated skull. These landmark sets were reassembled into a close approximation of the proper *in situ* arrangement, which we term the four opercular dataset (Figs 1B, 2B). Reassembly used two-point registration with two identical landmarks for each bone from the whole skull dataset. This procedure allowed us to examine the potential evolutionary role of shape, size, and orientation in the four-bone assemblage and its collective shape. The four bones that we examined in this dataset contribute prominently to three of the links of the four-bar lever: the interopercle to the ventral link, the preopercle to the fixed link, and the opercle and subopercle together to the opercular link.

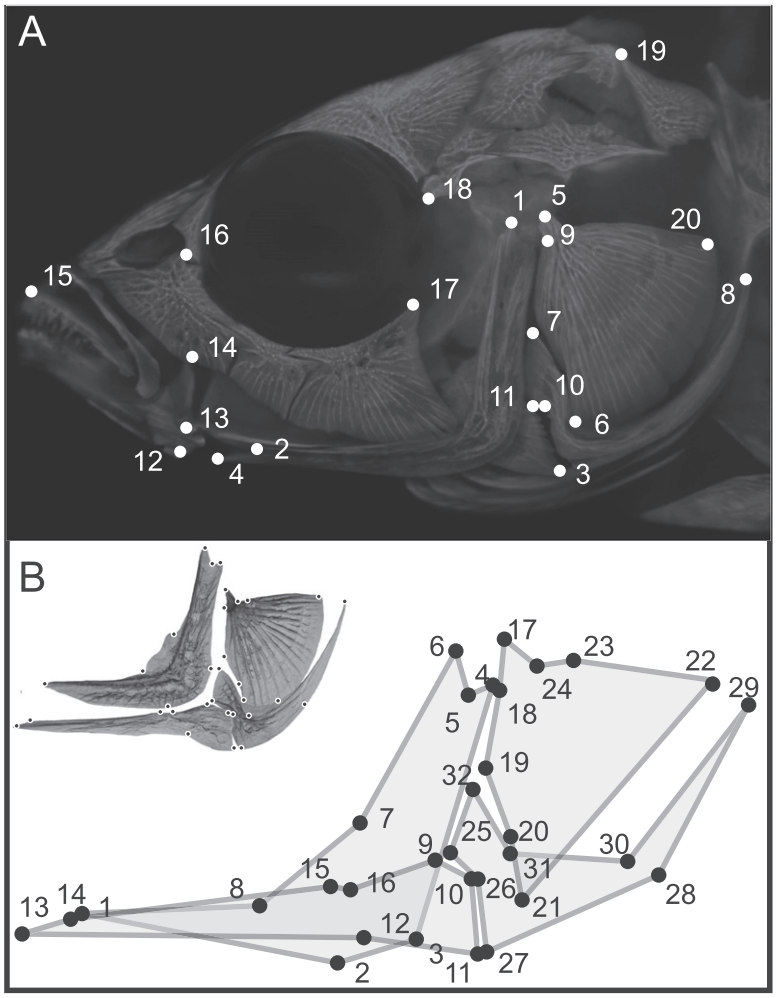

Figure 2. Two-dimensional landmark configuration, landmark numbers and detailed placement information for the whole-skull (A) and the four-bone datasets (B). In (B), the four opercular bones (opercle, subopercle, interopercle, preopercle; Fig. 1) were dissected out and landmarked individually to include points not present on the surface of the articulated skull. These landmark sets were reassembled into a close approximation of the proper *in situ* arrangement by two-point registration using two identical landmarks for each bone from the whole skull dataset.

The jaw link, not included in the four opercle data set, is within the mandible, extending from the retroarticular to the jaw joint.

All of the landmark sets described were digitized using TPSDIG, version 1.40 (Rohlf, 2001) and Procrustes-transformed using MORPHOJ, version 1.05d (Klingenberg, 2011).

Statistical analysis: shape, integration, and function

Covariance matrices were estimated from both the whole-skull and opercular four-bar lever landmark data, and several multivariate statistical techniques were applied to these datasets to assess variation in shape within and among our test populations, as well as the relationship of this variation to the opercular four-bar lever. Principal components analysis (PCA) was used to assess whole-skull, four opercular, and individual bone shape, and to ensure that the re-assembled four opercular configuration was accurately aligned. Differences in individual bone mean shape among populations were investigated using canonical variates analysis (CVA) of the Procrustes coordinates describing shape variation, and the significance of pairwise differences in mean shapes was assessed with permutation tests (10 000 rounds), using Procrustes distance as the test statistic. Discriminant function analysis (DFA) was also applied to these data to inquire whether it supported the CVA results.

Regression analysis was used to determine the amount of variation in shape in the whole-skull

configuration that could be explained by the mechanical efficiency of the opercular four-bar lever. Procrustes-transformed landmark configurations were regressed on centroid size, and the residuals from these regressions were then regressed on mechanical efficiency, represented in this analysis by transmission coefficient, to determine within- and among-group relationships between shape variation and feeding mechanics. These analyses were carried out on both unpooled data, and on data pooled by population.

Covariance matrix repeatability (t) was estimated for each population in the whole-skull dataset to determine the proportion of total variance in each group that results from individual variation (Cheverud, 1996b). The original datasets were resampled and covariance matrices re-estimated 1000 times, and the mean matrix correlation between these and the original datasets was taken as an estimate of t (Marroig & Cheverud, 2001). Similarity in global integration structure among populations in the whole-skull dataset was determined by computing correlations between covariation matrices and assessing significance using a permutation test. Observed correlations were then adjusted for small sample size using the formula $R_{adj} = R_{obs}/R_{max}$, where $R_{max} = (t_a t_b)^{1/2}$ (Marroig & Cheverud, 2001). Overall integration structure within each population was assessed by calculating the variance of the eigenvalues, standardized using the trace of the covariance matrix of the whole-skull configuration for each population (Wagner, 1984, 1990).

Integration structure within each dataset was assessed using Klingenberg's (2009) modularity analysis technique, based on partial least squares analysis (Rohlf & Corti, 2000), to compare patterns of covariation among landmarks in both the whole-skull and four opercular configurations. This technique employs the RV coefficient, which is a multivariate generalization of the squared correlation coefficient between two sets of variables. This metric measures covariation between two (or more) blocks of landmarks that were chosen based on a biological hypothesis of modular structure, and all other possible contiguous landmark partitions, scaled by the within-block variation (Klingenberg, 2009). If a hypothesized configuration indeed represents a modular arrangement of landmarks, then the RV coefficient should be among the lowest of all values calculated in the analysis.

The analyses described were performed in MORPHOJ, version 1.05d (Klingenberg, 2010) and JMP, version 8 (SAS Institute Inc.), except for the matrix repeatability calculations, which were performed in R (R Development Core Team, 2008).

RESULTS

Oceanic and lacustrine stickleback populations are differentiated by prominent shape changes in the opercular region of the skull

PCA of the complete skull dataset revealed that skull shapes of stickleback from both lakes have diverged from the oceanic form (Fig. 3A1, 2). The Boot Lake skull is moderately divergent along an axis previously associated with a limnetic (water column-feeding) morphology, elongated along the anteroposterior axis and narrower along the dorsoventral axis, represented here by PC1 (43% of variance explained; upper configuration in Fig. 3A1). The Bear Paw Lake skull is divergent in the same direction along PC1 as the Boot Lake skull. However, the Bear Paw Lake skull is less elongated along the anteroposterior axis, and is broader dorsoventrally, with these differences represented by PC2 (Fig. 3A2; 22% of variance explained; lower configuration in Fig. 3A1). These Bear Paw-specific features previously have been associated with a benthic (bottom-feeding) morphology (Fig. 3A). However, neither population exhibits strong divergence with respect to skull trophic morphology observed for stickleback from the same geographical region. These results agree with those reported previously (Willacker *et al.*, 2010), indicating that both populations retain a relatively generalized phenotype. There is also a general broadening and shortening in the preorbital region toward the Bear Paw Lake end of the PC2 axis that we do not consider further here.

PCA of the shapes of the four individual opercular bones, representing three links of the opercular four-bar lever (see Material and Methods), reveals that all of the bones have evolved in somewhat different directions (see Supporting information, Fig. S1). CVA supports that each population has reached a new average shape for each bone ($P < 0.0001$ for all comparisons; data not shown). Similarly, DFA revealed no misclassifications using either the discriminant scores or the cross-validation scores in pairwise comparisons of the three populations (data not shown). PCA of the collective shape of the four opercular bone set (Fig. 3B2), in which the sizes and orientations of the individual bones are preserved, is consistent with the major trends observed for the complete skull dataset (Fig. 3A2). Moreover, this analysis of the four opercular bone set reveals two prominent deformations along PC1 (36% of variance explained). One, considering the evolutionary change toward the lake populations (toward negative PC1), is a dorsally located anteroposterior expansion, discovered previously for the opercle (Kimmel *et al.*, 2008), and now shown to encompass the neighbouring bones in this region: the preopercle and the subopercle (Fig. 3B1, asterisk). The

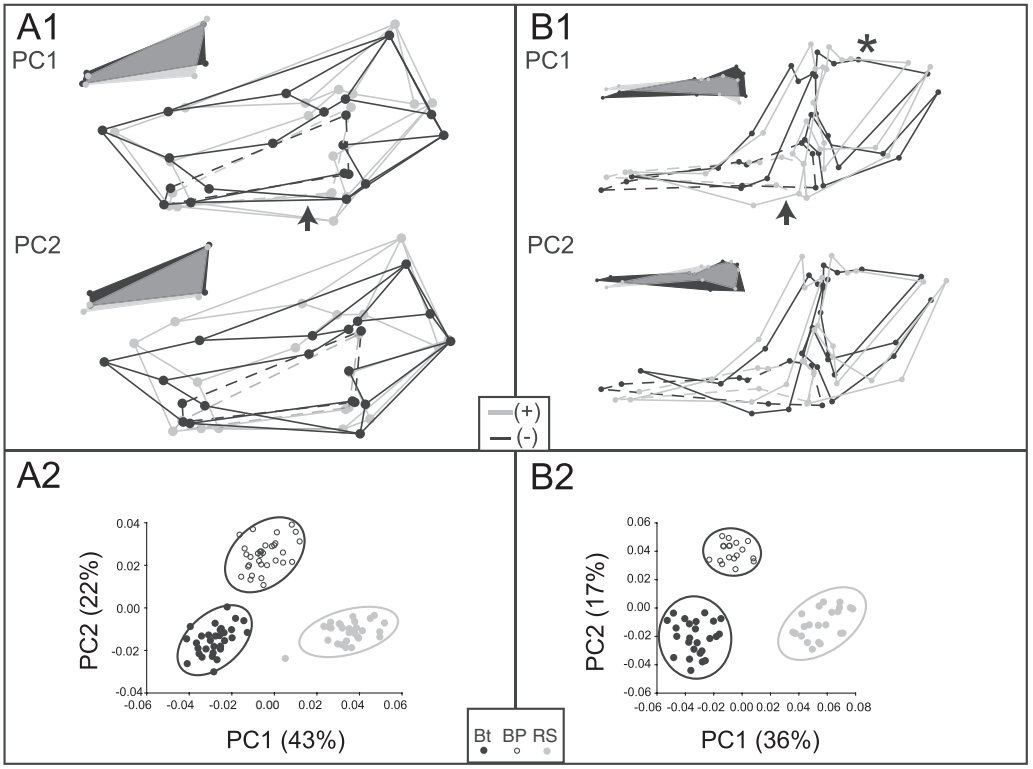

Figure 3. Principal component (PC) analysis of (A) the whole skull and (B) the four opercular bone landmark configurations. In (A1) and (B1), the black wireframes indicate the negative end of the principal component axis, whereas grey wireframes indicate the positive end. Dashed lines and insets in (A1) indicate the approximate location of the opercular four-bar lever. Dashed lines and insets in (B1) indicate the interopercle bone within the configuration. In (A2) and (B2), percentages indicated on PC axes indicate the percentage of total variance explained by each PC. Ellipses represent 95% equal frequency ellipses for each population. An asterisk indicates dorsal region expansion; arrows indicate ventral region expansion. BP, Bear Paw Lake; Bt, Boot Lake; RS, Rabbit Slough.

second and most prominent deformation of the entire four-opercular bone configuration is also a local anteroposterior expansion, located at a ventral position. A stretching out along the anteroposterior axis of the posterior region of interopercle and associated preopercle can be seen clearly (Fig. 3B1, arrow). This ventral region expansion also manifests as a prominent deformation with the complete skull dataset (Fig. 3A1, arrow). Immediately anterior to the location of the ventral expansion, the interopercle connects via a ligament with the underlying ceratohyal bone. Immediately to either side of the expansion, two compressions of the configuration occur: the anterior, including the interopercle and the preopercle, and the posterior, including the opercle compression discovered previously (Kimmel *et al*., 2008), and encompassing the subopercle (Fig. 3B1).

The transmission coefficient of the four-bar lever is strongly correlated with the major axes of skull shape variation

Comparisons of the shapes of the opercular four-bar lever among the three populations show that the lever organization has evolved substantially in the Boot Lake fish, where the size-standardized lengths of all four links of the lever are significantly different from those of the population representing the marine ancestor (Rabbit Slough; Fig. 4A). The resulting transmission coefficient of the Boot Lake fish is significantly reduced (Fig. 4B). By contrast, for the Bear Paw Lake fish, only the opercular link is significantly different (lower) from Rabbit Slough, and transmission coefficient is not significantly different from that of Rabbit Slough.

Regression of variation in skull shape, which was derived from the complete skull landmark configuration, against transmission coefficient reveals a large proportion of the variance in shape observed in all three populations explained by transmission coefficient ($P < 0.0001$) (Fig. 5), both when specimens are not pooled (13.6%) (Fig. 5A) and when specimens are pooled by population (14.2%) (Fig. 5B). Low transmission coefficient values correspond to an elongated anteroposterior axis and a narrowed dorsoventral axis, and high transmission coefficient values correspond to a less elongated anteroposterior axis and a

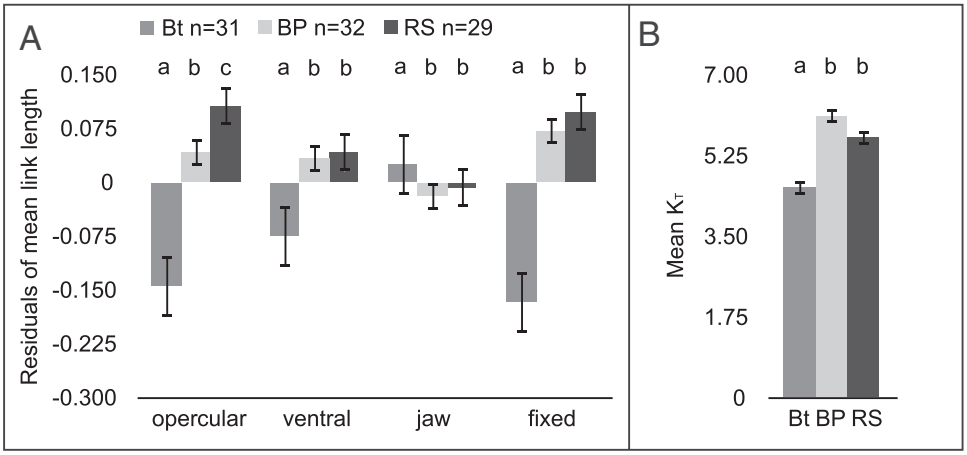

Figure 4. Biomechanical assessment of the components of the four-bar lever in three populations of threespine stickleback, including (A) opercular four-bar link lengths and (B) transmission coefficient. Opercular four-bar link lengths (residuals of mean ± SE link length) are size-standardized by taking the residuals from ordinary least squares linear regression on fish standard length. Groups not connected by the same letter are significantly different ($P < 0.0500$; Tukey–Kramer comparison of means). BP, Bear Paw Lake; Bt, Boot Lake; K_T, transmission coefficient (1/mechanical efficiency); *N*, number of specimens; RS, Rabbit Slough.

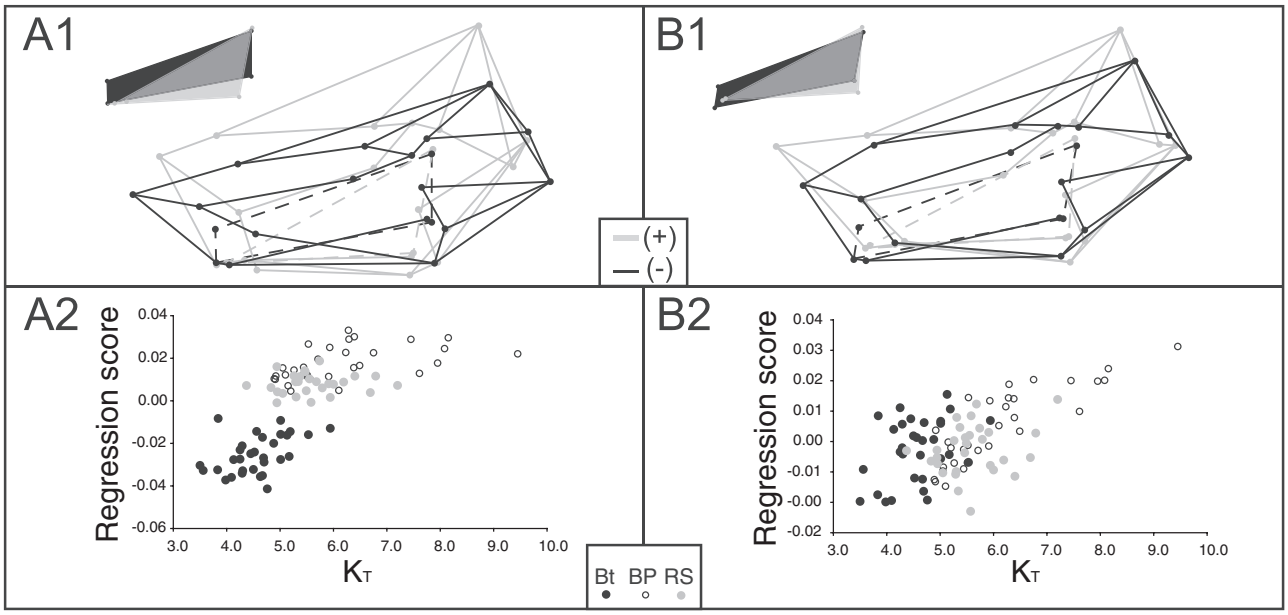

Figure 5. Regression analysis of the whole skull using unpooled data (A) and data pooled by population (B). In (A1) and (B1), the black wireframes indicate the negative end of the transmission coefficient (K_T) axis, whereas grey wireframes indicate the positive end. Dashed lines and insets in (A1) and (B1) indicate the approximate location of the opercular four-bar lever. BP, Bear Paw Lake; Bt, Boot Lake; RS, Rabbit Slough.

broader dorsoventral axis. In the unpooled dataset, the three populations cluster in different regions of the regression, with Boot Lake individuals residing at lower transmission coefficient values, whereas Bear Paw Lake and Rabbit Slough cluster at higher transmission coefficient values.

Evolutionary change predicts a key component of a complex modular organization

Covariance matrix repeatability is high across all three populations, and adjusted matrix correlations for all possible pairwise comparisons are large and

Table 1. Covariance matrix comparison among populations for the whole-skull dataset

	Boot Lake	Bear Paw Lake	Rabbit Slough
Boot Lake	**0.8153**	0.8817	0.9021
Bear Paw Lake	0.7366	**0.8570**	0.7931
Rabbit Slough	0.6491	0.5850	**0.6349**

Matrix repeatability (t) is given in bold along the diagonal, with raw correlations below and adjusted correlations above. All correlations are highly significant ($P < 0.0001$).

Table 2. Scaled variance of eigenvalues and SDs of the variance–covariance matrix for the whole-skull landmark configuration in three populations of threespine stickleback

Population	Scaled variance of Eigenvalues	SD
Rabbit Slough	0.0012	0.0002
Boot Lake	0.0013	0.0001
Bear Paw Lake	0.0013	0.0002

highly significant ($P < 0.0001$) (Table 1), indicating that all three populations exhibit similar phenotypic covariance structure for this landmark configuration. The scaled variance of eigenvalues is similar across all three populations, indicating that the magnitude of integration within each covariance matrix is similar (Table 2).

Hypothesizing that evolutionary change is influenced by skull modularity predicts that the ventral region expansion recovered in both the full skull and four opercular bone data sets could correspond to a boundary between developmental modules. Modularity hypothesis testing of both of these configurations shows that, within the three-population dataset as a whole, there exists a boundary near the middle of the opercular region that divides the landmarks into anterior and posterior modules (Fig. 6A, B, Table 3). In the four bone configuration, the boundary crosses the configuration and subdivides the interopercle and preopercle together, just posterior to where the interopercle makes a ligamentous connection to the interhyal (at landmark 15 in the four opercular set) (Figs 2, 6B). This boundary occurs, as predicted, precisely within the ventral region revealed by PCA to have undergone a prominent evolutionary anteroposterior expansion. The same module boundary is also recovered in the four opercular set evaluated for each population independently, and in the whole-skull set for Boot Lake and Rabbit Slough (Table 4), further supporting the presence of similar covariation structure across all three populations. Also illustrating the complexity of integration structure, we note that the opercle is itself a module within the four opercular configuration (Fig. 6C, Table 3). If the configuration is split into not just two but four blocks, then each bone is also revealed to be a separate module (Fig. 6D, Table 3).

DISCUSSION

The focus of the present study was to learn how morphology and function in the opercular region of the skull of divergent stickleback populations are associated with one another, and how skull integration structure might impact this association. A key finding is that shape variation in the skull explains a large proportion of the variation in the transmission coefficient of the opercular four-bar lever. This correlation supports the hypothesis that feeding mechanics influence the evolution of skull shape. We observed that modularity in the opercular four-bar region of the skull is complex. Modules are overlapping, in accordance with the palimpsest hypothesis (Hallgrimsson *et al*., 2009) that posits that modularity is sequentially generated by the spatiotemporal organization of developmental processes. In particular, we find a strongly supported module boundary passing through the set of opercular bones in exactly the position predicted by a prominent shape deformation that contributes to the major axis of evolutionary change (PC1) between the oceanic and two lacustrine populations in the present study. Our data suggest, furthermore, that this boundary has been conserved among all three populations. This finding argues strongly against the 'modular absence' hypothesis and for the 'modular stasis' hypothesis, and also suggests that 'modular reorganization' among these populations is not a feature of the evolutionary divergence that we examine. The association between conserved skull modularity and substantial evolutionary divergence can be taken as support for developmental bias positively influencing, or at least not constraining, evolutionary change.

How might modularity impact evolutionary change?

As revealed by multivariate regression of skull shape on the opercular four-bar lever transmission coefficient, structure–function correlation is strong and highly significant. Strikingly, and with respect to the four-bar lever shape specifically, the major axes of shape variation represented by the regression match the major axes of shape variation revealed by PCA (Fig. 7A). One end of the regression axis matches

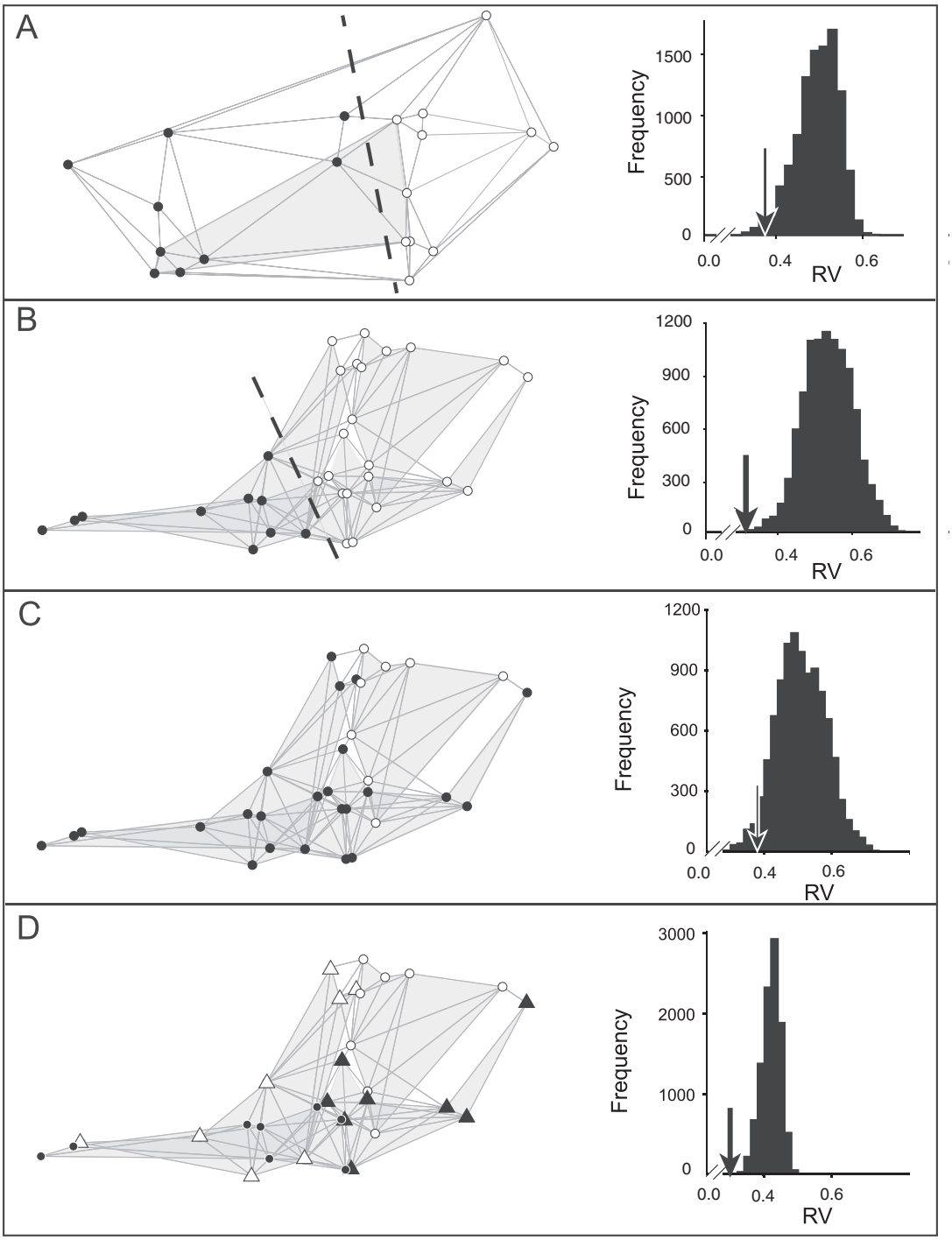

Figure 6. Modular structure of the whole skull and four opercular bone landmark configurations. The anteroposterior modular boundary is shown in the whole skull (A) and the four opercular bone landmark configurations (B). (C, the opercle is supported as a module, and each of the four opercular bones (D) is supported as individual modules within the four opercular bone configuration. Landmark shapes and fills indicate assignment to different modules. The shaded polygon in (A) indicates the approximate location of the opercular four-bar lever. The shaded polygons in (B), (C), and (D) indicate the anatomical locations of the four opercular bones within the configuration (for details, see text and Figs 1, 2). Arrows indicate the RV value for the hypothesized modular arrangement, within the complete distribution of RV values for possible modular arrangements. For details on this value, see Klingenberg (2009).

Table 3. Modularity analysis of the whole-skull and four opercular landmark configurations in three populations of threespine stickleback

Hypothesis	Whole skull	4OP
Anteroposterior split	0.3741/0.0172	0.3152/0.0000
Opercle	–	0.3796/0.0313
All four bones	–	0.2985/0.0000

Values reported are in the form RV/proportion lower, where the proportion lower is essentially equivalent to a *P*-value (Klingenberg, 2009).
AP split, anteroposterior division into two modules; 4OP, four opercular dataset. For details on hypothesis determination, see Material and Methods.

Table 4. Assessment of the presence of an anterior-posterior module boundary, by population, of the whole-skull and four opercular landmark configurations in three populations of threespine stickleback

	Whole skull	4OP
Boot Lake	0.5195/0.0335	0.5185/0.0180
Bear Paw Lake	0.6512/0.2678	0.4736/0.0170
Rabbit Slough	0.3754/0.0136	0.3679/0.0020

Values reported are in the form RV/proportion lower, where the proportion lower is essentially equivalent to a *P*-value (Klingenberg, 2009). The shaded cell indicates a module that is not supported.
4OP, four opercular dataset. For details on hypothesis determination, see Material and Methods.

evolutionary change along PC1, and the other end along PC2. We conclude that variation in function of the opercular four-bar lever is therefore directly related to important aspects of evolutionary variation in shape of this region of the skull between oceanic and lake sticklebacks.

We propose a novel model for how conserved modularity in this skull region might have influenced this structural and functional evolutionary change. As explained in the Introduction, one of the opercular bones, the interopercle, is directly involved not only in the opercular four-bar lever apparatus, but also in a second mechanical system driving jaw opening, the mandibular–hyoid linkage. Because the sternohyoid muscle, which effects jaw movement through the hyoid linkage, is much larger in cross-sectional area than the opercular levator muscle, this hyoid linkage has the potential to deliver greater force to mandibular rotation than the opercular four-bar lever (Anker, (1974); de Visser & Barel (1998); Durie & Turingan (2004)). The interopercle connects to the retroarticular process of the lower jaw through a ligament at its anterior end (at landmark 13) (Fig. 7B) and to the underlying ceratohyal of the hyoid linkage at another ligament part way along its shaft (at landmark 15). Both of these ligamentous connections are anterior to the conserved module boundary and, critically for our model, we observe that only slight evolutionary changes occur in the relative positions of these two connections (Fig. 7B). This invariance implies strong conservation of shape and function of the hyoid–mandibular linkage, apparently independently of changes that occur in the four-bar apparatus. Because Boot Lake and Bear Paw Lake stickleback populations show prominent change in the same direction along PC1, the hyoid linkage would be conserved in both, despite relatively marked divergence in opercular four-bar lever mechanics between them. The anterior–posterior stretching out of the interopercle in its posterior region specifically, which is the region crossed by the module boundary (Fig. 7B), coupled with the associated dorsoventral narrowing of the subopercle and opercle (in the Boot Lake fish particularly), alters the shape of the opercular four-bar lever system that transmits opercular rotation to the mandible through the interopercle. The shorter opercular link (opercle and subopercle), along with the observed changes in the other four-bar links, result in a system that transmits more force and less movement, a modification that would allow more forceful jaw depression. We propose that it is the integration structure of this apparatus, specifically that the anterior and posterior margins are internally integrated at the same time as being substantially modular with respect to one another, that allows functionally significant shape change in response to directional selection toward a lacustrine morphology to occur along a labile intermediate region.

The idea of a boundary region that is labile with respect to evolutionary change in shape matches our recent finding that a module boundary passes within the stickleback opercle bone. We found that the position of the boundary correlated with the way the single bone deforms in shape during evolution between the oceanic and lacustrine form (Kimmel *et al*., 2012). Considering both results together supports a proposition that modularity permits dissociability (Needham, 1933) and thus facilitates shape evolution. In the present study, we see a correlated shape deformation of two adjacent bones, fitting a principle that modularity might facilitate both the coupling and decoupling of traits (Young & Hallgrimsson, 2005). For at least the shape of the opercle, and likely for the other elements of the opercular four-bar lever as well, evolution can occur extremely quickly, as measured in tens of years rather

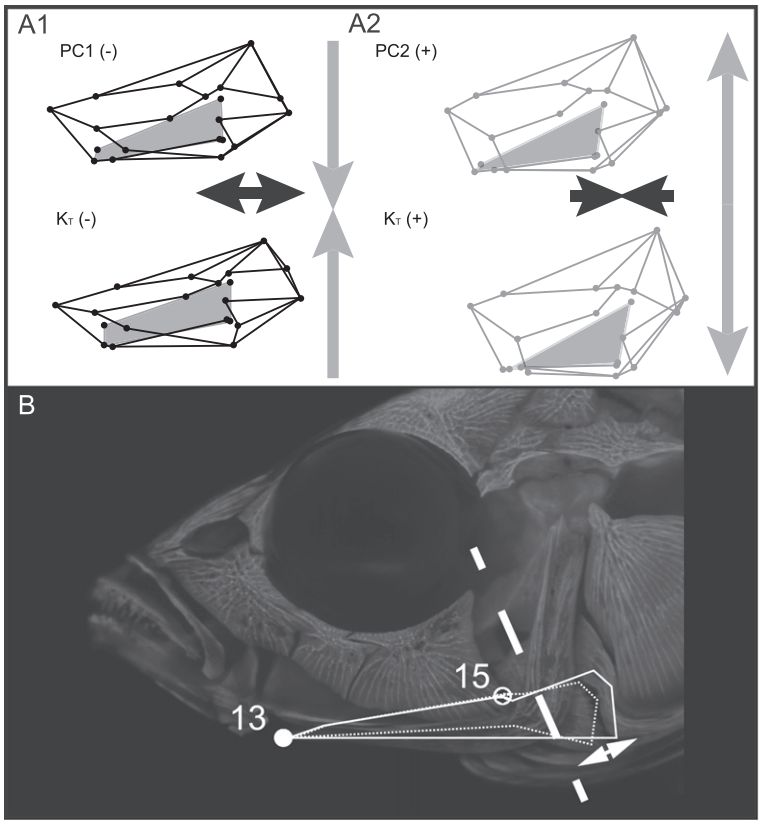

Figure 7. A, comparison of results from our analyses of shape variation, shape variation in relation to mechanical efficiency, and modularity hypothesis testing, using the whole-skull configuration. In (A1) and (A2), the black wireframes indicate the negative end of the principal component (PC) or transmission coefficient (K_T) axis, whereas grey wireframes indicate the positive end. Shaded polygons in (A1) and (A2) indicate the approximate location and shape of the opercular four-bar lever. In (A1) and (A2), black arrows indicate anteroposterior shape variation; grey arrows indicate dorsoventral shape variation. B, location of ligamentous attachments of the interopercle, illustrated on the side view of the skull. Here, the interopercle deformation has been extracted from the Procrustes superimposition and has been aligned to the skull using landmarks 13 and 15 (Fig. 2B). In (B), the solid circle (landmark 13) indicates the approximate location of the ligamentous connection of the interopercle to the jaw; the open circle (landmark 15) indicates the approximate location of the ligamentous connection of the interopercle to the ceratohyal; and the dashed line indicates the location of the ventral region anteroposterior modular boundary described (for details, see Fig. 6). Polygons in (B) indicate the location of the interopercle and its shape deformation, highlighted by the white arrow.

than thousands or millions of years (Arif, Aguirre & Bell, 2009; Kimmel *et al.*, 2012). It is tempting to speculate that modularity is a key feature in this example of rapid evolutionary change. A similar role for modularity has been proposed recently for the oral jaws of cichlid fishes (Parsons, Cooper & Albertson, 2011), which demonstrate similarly rapid adaptive divergence in trophic morphology.

Implications of conservation and apparent complexity of modular architecture

Partially independent functional linkages that operate in the hyomandibular region of the skull may be linked to skull integration structure and modularity. Our evidence also suggests that, in this system, modularity is complex, with at least two distinctive modular patterns showing up within the same set of four opercular bones: the module boundary that passes across the interopercle and preopercle is within a pair of adjacent skull elements, and not between elements. In a second, independent test of modularity, each of the bones in the set of four behaves as a single module. The two module patterns overlap such that one is not neatly nested within the other. This composite structure is as predicted by the palimpsest hypothesis, in which the two patterns would arise at different developmental stages (Hallgrimsson *et al.*, 2009). We can

predict the order. The earliest bone ossifications show individuality, being only a few cell diameters in size and appearing at somewhat remote locations from one another and at separate developmental times (Kimmel *et al*., 2005; 2010; Eames *et al*., 2013). Regulation of patterning at such early developmental stages depends on conserved intercellular signalling between cells, and read-out of the signals by transcription factors (Klingenberg, 2008, 2010; Huycke, Eames & Kimmel, 2012). Functional associations (e.g. articulations) between the neighbouring bones arise only later, when, through continued bone outgrowth and enlargement, the developing bone rudiments come to be connected or overlapped with one another (e.g. the interopercle and preopercle). Hence, understanding the developmental trajectory predicts that modular patterns involving such functional association will arise later than the pattern in which bones are unitary. Assuming that modularity can be assessed during the appropriate developmental stages, this hypothesis can be tested directly.

Our analysis suggests that the developmental architecture underlying the modularity is shared within the populations examined. The oceanic and lake populations all exhibit conserved phenotypic covariance structure, and we see modular stasis when we evaluate modularity separately for each population. The fact that the modularity pattern is conserved among our populations may also be significant in light of the palimpsest model. As stated previously, the model predicts that covariance structure among traits can change significantly simply by alterations in the relative amounts of variance in developmental processes that generate covariance (Hallgrimsson *et al*., 2009). In the context of a complex 'palimpsest' pattern of modularity in the stickleback skulls, our observation of conservation of a modularity pattern implies not only the conservation of skull developmental architecture, but also the relative stability of variance in the processes that generate the skull covariance structure. The conservation of covariance structure may reflect the effects of selection for jaw function that require the maintenance of structure–function relationships across a range of variation in cranial shape.

The conserved modular organization of the anterior and posterior regions of the hyomandibular portion of the skull in oceanic and freshwater stickleback has several potential explanations. This modular organization may be an ancestral trait that exists outside of the stickleback lineage. If so, this integrated architecture could bias or constrain the direction of evolution along the boundary that we document in the present study, irrespective of the optimal phenotype combinations imposed by the habitats. This is a testable hypothesis that predicts a similar craniofacial modularity in more distantly-related fishes that occupy different habitats. Alternatively, the modular organization itself could be a derived feature of the stickleback lineage. Recent molecular population genetic evidence (Colosimo *et al*., 2005; Hohenlohe *et al*., 2010; 2012; Jones *et al*., 2012) makes clear that, although any particular freshwater population may be quite young, genetic variation that is important for adaptation to each habitat may be very old as a result of extensive, long-term gene flow between oceanic and freshwater habitats (Schluter & Conte, 2009). A testable hypothesis is therefore that the modularity may have evolved in response to spatially-mediated balancing selection on a fitness landscape with divergent oceanic and freshwater optima. In this context, it is important to note that we recovered the module boundary splitting the opercular four-bar lever in the Rabbit Slough population examined alone, and not just in the combined oceanic and lake dataset. A metapopulation scenario such as appears to be the case in stickleback could lead to the evolution of modular genetic architecture that aligns with the adaptive landscape and facilitates the rapid evolution observed in this species.

ACKNOWLEDGEMENTS

The research presented here was supported by NSF grant IOS-0818738 to CBK and WAC, and in part by an NSERC Discovery Grant to HAJ. We are grateful to the members of the Kimmel and Cresko labs for comments on earlier versions of this work, and to C. Klingenberg and three anonymous reviewers for insightful comments that helped to improve the quality of this manuscript.

REFERENCES

Aguirre WE, Bell MA. 2012. Twenty years of body shape evolution in a threespine stickleback population adapting to a lake environment. *Biological Journal of the Linnean Society* **105:** 817–831.

Albertson RC, Streelman JT, Kocher TD, Yelick PC. 2005. Integration and evolution of the cichlid mandible: the molecular basis of alternate feeding strategies. *Proceedings of the National Academy of Sciences of the United States of America* **102:** 16287–16292.

Anker GC. 1974. Morphology and kinetics of the head of the stickleback, *Gasterosteus aculeatus*. *Transactions of the Zoological Society of London* **32:** 311–416.

Anker GC. 1985. The morphology of joints and ligaments in the head of a generalized haplochromis species: *H. elegans* Trewavas 1933 (Teleostei, Cichlidae). *Netherlands Journal of Zoology* **36:** 498–529.

Arif S, Aguirre WE, Bell MA. 2009. Evolutionary diversification of opercle shape in Cook Inlet threespine stickleback. *Biological Journal of the Linnean Society* **97:** 832–844.

Atchley W, Hall B. 1991. A model for development and evolution of complex morphological structures. *Biological Reviews of the Cambridge Philosophical Society* **66:** 101–157.

Bell MA, Foster SA. 1994. *The evolutionary biology of the threespine stickleback*. New York, NY: Oxford University Press.

Cheverud JM. 1982. Phenotypic, genetic, and environmental morphological integration in the cranium. *Evolution* **36:** 499–516.

Cheverud JM. 1996a. Developmental integration and the evolution of pleiotropy. *Integrative and Comparative Biology* **36:** 44–50.

Cheverud JM. 1996b. Quantitative genetic analysis of cranial morphology in the cotton-top (*Saguinus oedipus*) and saddle-back (*S. fuscicollis*) tamarins. *Journal Of Evolutionary Biology* **9:** 5–42.

Colosimo PF, Hosemann KE, Balabhadra S, Villareal G Jr, Dickson M, Grimwood J, Schmutz J, Myers RM, Schluter D, Kingsley DM. 2005. Widespread parallel evolution in sticklebacks by repeated fixation of ectodysplasin alleles. *Science* **307:** 1928–1933.

Cresko WA, Amores A, Wilson C, Murphy J, Currey M, Phillips P, Bell MA, Kimmel CB, Postlethwait JH. 2004. Parallel genetic basis for repeated evolution of armor loss in Alaskan threespine stickleback populations. *Proceedings of the National Academy of Sciences of the United States of America* **101:** 6050–6055.

Cresko WA, Baker JA. 1996. Two morphotypes of lacustrine threespine stickleback, *Gasterosteus aculeatus*, in Benka Lake, Alaska. *Environmental Biology of Fishes* **45:** 343–350.

Darwin CR. 1859. *On the origin of species by means of natural selection*. London: John Murray.

Durie CJ, Turingan RG. 2004. The effects of opercular linkage disruption on prey-capture kinematics in the teleost fish *Sarotherodon melanotheron*. *Journal of Experimental Zoology* **301A:** 642–653.

Eames BF, DeLaurier A, Ullmann B, Huycke TR, Nichols JT, Dowd J, McFadden M, Sasaski MM, Kimmel CB. 2013. FishFace: interactive atlas of zebrafish craniofacial development at cellular resolution. *BMC Developmental Biology* **13:** 23.

Fish JL, Villmoare B, Köbernick K, Compagnucci C, Britanova O, Tarabykin V, Depew MJ. 2011. Satb2, modularity, and the evolvability of the vertebrate jaw. *Evolution and Development* **13:** 549–564.

Goswami A. 2006. Cranial modularity shifts during mammalian evolution. *The American Naturalist* **168:** 270–280.

Hallgrimsson B, Jamniczky HA, Young NM, Rolian C, Parsons TE, Boughner JC, Marcucio RS. 2009. Deciphering the palimpsest: studying the relationship between morphological integration and phenotypic covariation. *Evolutionary Biology* **36:** 355–376.

Hallgrimsson B, Lieberman DE, Liu W, Ford-Hutchinson AF, Jirik FR. 2007a. Epigenetic interactions and the structure of phenotypic variation in the cranium. *Evolution and Development* **9:** 76–91.

Hallgrimsson B, Lieberman DE, Young NM, Parsons TE, Wat S. 2007b. Evolution of covariance in the mammalian skull. *Novartis Foundation Symposium* **284:** 164–185.

Hansen TF, Houle D. 2008. Measuring and comparing evolvability and constraint in multivariate characters. *Journal of Evolutionary Biology* **21:** 1201–1219.

Hendrikse JL, Parsons TE, Hallgrimsson B. 2007. Evolvability as the proper focus of evolutionary developmental biology. *Evolution and Development* **9:** 393–401.

Hohenlohe PA, Bassham S, Currey M, Cresko WA. 2012. Extensive linkage disequilibrium and parallel adaptive divergence across threespine stickleback genomes. *Philosophical Transactions of the Royal Society of London Series B, Biological Sciences* **367:** 395–408.

Hohenlohe PA, Bassham S, Etter PD, Stiffler N, Johnson EA, Cresko WA. 2010. Population genomics of parallel adaptation in threespine stickleback using sequenced RAD tags. *PLoS Genetics* **6:** e1000862.

Hulsey CD, Fraser GJ, Streelman JT. 2005. Evolution and development of complex biomechanical systems: 300 million years of fish jaws. *Zebrafish* **2:** 243–257.

Huycke TR, Eames BF, Kimmel CB. 2012. Hedgehog-dependent proliferation drives modular growth during morphogenesis of a dermal bone. *Development* **139:** 2371–2380.

Jamniczky HA, Hallgrimsson B. 2009. A comparison of covariance structure in wild and laboratory muroid crania. *Evolution* **63:** 1540–1556.

Jamniczky HA, Hallgrimsson B. 2011. Modularity in the skull and cranial vasculature of laboratory mice: implications for the evolution of complex phenotypes. *Evolution and Development* **13:** 28–37.

Jamniczky HA, Harper EE, Garner R, Cresko WA, Wainwright PC, Hallgrímsson B, Kimmel CB. 2013. Data from: association between integration structure and functional evolution in the opercular four-bar apparatus of the threespine stickleback, *Gasterosteus aculeatus* (Pisces: Gasterosteidae). *Dryad Digital Repository*. doi:10.5061/dryad.4b5c4.

Jones AG, Arnold SJ, Bürger R. 2007. The mutation matrix and the evolution of evolvability. *Evolution* **61:** 727–745.

Jones FC, Grabherr MG, Chan YF, Russell P, Mauceli E, Johnson J, Swofford R, Pirun M, Zody MC, White S, Birney E, Searle S, Schmutz J, Grimwood J, Dickson MC, Myers RM, Miller CT, Summers BR, Knecht AK, Brady SD, Zhang H, Pollen AA, Howes T, Amemiya C, Baldwin J, Bloom T, Jaffe DB, Nicol R, Wilkinson J, Lander ES, Di Palma F, Lindblad-Toh K, Kingsley DM. 2012. The genomic basis of adaptive evolution in threespine sticklebacks. *Nature* **484:** 55–61.

Kassen R, Schluter D, McPhail JD. 1995. Evolutionary history of threespine sticklebacks (*Gasterosteus* spp.) in British Columbia: insights from a physiological clock. *Canadian Journal of Zoology* **73:** 2154–2158.

Kimmel CB, Aguirre WE, Ullmann B, Currey M, Cresko WA. 2008. Allometric change accompanies opercular shape evolution in Alaskan threespine sticklebacks. *Behaviour* **145:** 669–691.

Kimmel CB, Cresko WA, Phillips PC, Ullmann B, Currey M, Hippel F, Kristjánsson BK, Gelmond O, McGuigan K. 2012. Independent axes of genetic variation and parallel evolutionary divergence of opercle bone shape in threespine stickleback. *Evolution* **66:** 419–434.

Kimmel CB, DeLaurier A, Ullmann B, Dowd J, McFadden M. 2010. Modes of developmental outgrowth and shaping of a craniofacial bone in zebrafish. *PLoS ONE* **5:** e9475.

Kimmel CB, Ullmann B, Walker C, Wilson C, Currey M, Phillips PC, Bell MA, Postlethwait JH, Cresko WA. 2005. Evolution and development of facial bone morphology in threespine sticklebacks. *Proceedings of the National Academy of Sciences of the United States of America* **102:** 5791–5796.

Kingsley DM, Zhu B, Osoegawa K, De Jong PJ, Schein J, Marra M, Peichel C, Amemiya C, Schluter D, Balabhadra S. 2004. New genomic tools for molecular studies of evolutionary change in threespine sticklebacks. *Behaviour* **141:** 11–12.

Klingenberg CP. 2008. Morphological integration and developmental modularity. *Annual Review of Ecology Evolution and Systematics* **39:** 115–132.

Klingenberg CP. 2009. Morphometric integration and modularity in configurations of landmarks: tools for evaluating a priori hypotheses. *Evolution and Development* **11:** 405–421.

Klingenberg CP. 2010. Evolution and development of shape: integrating quantitative approaches. *Nature Reviews Genetics* **11:** 623–635.

Klingenberg CP. 2011. MORPHOJ: an integrated software package for geometric morphometrics. *Molecular Ecology Resources* **11:** 353–357.

Klingenberg CP, Duttke S, Whelan S, Kim M. 2012. Developmental plasticity, morphological variation and evolvability: a multilevel analysis of morphometric integration in the shape of compound leaves. *Journal of Evolutionary Biology* **25:** 115–129.

Lande R. 1979. Quantitative genetic analysis of multivariate evolution, applied to brain: body size allometry. *Evolution* **42:** 467–481.

Lauder GV. 1985. Aquatic feeding in lower vertebrates. In: Hildebrand M, Bramble DM, Liem KF, Wake DB, eds. *Functional vertebrate morphology*. Cambridge, MA: Belknap Press, 210–229.

Lavin PA, McPhail JD. 1985. The evolution of freshwater diversity in the threespine stickleback (*Gasterosteus aculeatus*): site-specific differentiation of trophic morphology. *Canadian Journal of Zoology* **63:** 2632–2638.

Lavin PA, McPhail JD. 1986. Adaptive divergence of trophic phenotype among freshwater populations of the threespine stickleback (*Gasterosteus aculeatus*). *Canadian Journal of Fisheries and Aquatic Sciences* **43:** 2455–2463.

Lavin PA, McPhail JD. 1987. Morphological divergence and the organization of trophic characters among lacustrine populations of the threespine stickleback (*Gasterosteus aculeatus*). *Canadian Journal of Fisheries and Aquatic Sciences* **44:** 1820–1829.

Liem KF. 1970. Comparative functional anatomy of the Nandidae (Pisces: Teleostei). *Fieldiana: Zoology* **56:** 1–166.

Liem KF. 1974. Evolutionary strategies and morphological innovations: cichlid pharyngeal jaws. *Systematic Zoology* **22:** 425–441.

Marroig G, Cheverud JM. 2001. A comparison of phenotypic variation and covariation patterns and the role of phylogeny, ecology, and ontogeny during cranial evolution of New World monkeys. *Evolution* **55:** 2576–2600.

McPhail JD. 1984. Ecology and evolution of sympatric sticklebacks (*Gasterosteus*): morphological and genetic evidence for a species pair in Enos Lake, British Columbia. *Canadian Journal of Zoology* **62:** 1402–1408.

McPhail JD. 1993. Ecology and evolution of sympatric sticklebacks (*Gasterosteus*): origin of the species pairs. *Canadian Journal of Zoology* **71:** 515–523.

Muller M. 1996. A novel classification of planar four-bar linkages and its application to the mechanical analysis of animal systems. *Philosophical Transactions Biological Sciences* **351:** 689–720.

Needham J. 1933. On the dissociability of the fundamental processes in ontogenesis. *Biological Reviews* **8:** 180–223.

Olson RC, Miller RL. 1958. *Morphological integration*. Chicago, IL: University of Chicago Press.

Parnell NF, Hulsey CD, Streelman JT. 2012. The genetic basis of a complex functional system. *Evolution* **66:** 3352–3366.

Parsons KJ, Cooper WJ, Albertson RC. 2011. Modularity of the oral jaws is linked to repeated changes in the craniofacial shape of African cichlids. *International Journal of Evolutionary Biology* **2011:** 1–10.

Parsons KJ, Márquez E, Albertson RC. 2012. Constraint and opportunity: the genetic basis and evolution of modularity in the cichlid mandible. *American Naturalist* **179:** 64–78.

R Development Core Team. 2008. R: a language and environment for statistical computing. Available at: http://www.r-project.org/

Raff RA. 1996. *The shape of life*. Chicago, IL: University of Chicago Press.

Rohlf FJ. 2001. *tpsDig*. Available at: http://life.bio.sunysb.edu/morph/index.html

Rohlf FJ, Corti M. 2000. Use of two-block partial least-squares to study covariation in shape. *Systematic Biology* **49:** 740–753.

Sanger TJ, Mahler DL, Abzhanov A, Losos JB. 2011. Roles for modularity and constraint in the evolution of cranial diversity among anolis lizards. *Evolution* **66:** 1525–1542.

Schluter D, Conte GL. 2009. Genetics and ecological speciation. *Proceedings of the National Academy of Sciences of the United States of America* **106:** Suppl 1: 9955–9962.

Schluter D, Marchinko KB, Barrett RDH, Rogers SM. 2010. Natural selection and the genetics of adaptation in threespine stickleback. *Philosophical Transactions of the Royal Society of London Series B, Biological Sciences* **365:** 2479–2486.

Thompson DW. 1917. *On growth and form*. Cambridge: Cambridge University Press.

Tokita M, Kiyoshi T, Armstrong KN. 2007. Evolution of craniofacial novelty in parrots through developmental modularity and heterochrony. *Evolution and Development* **9:** 590–601.

Van Wassenbergh S, Herrel A, Adriaens D, Aerts P. 2005. A test of mouth-opening and hyoid-depression mechanisms during prey capture in a catfish using high-speed cineradiography. *Journal of Experimental Biology* **208:** 4627–4639.

de Visser J, Barel CDN. 1998. The expansion apparatus in fish heads, a 3-D kinetic deduction. *Netherlands Journal of Zoology* **48:** 361–395.

Wagner GP. 1984. On the eigenvalue distribution of genetic and phenotypic dispersion matrices: evidence for a non-random origin of quantitative genetic variation. *Journal of Mathematical Biology* **21:** 77–95.

Wagner GP. 1990. A comparative study of morphological integration in *Apis mellifera* (Insecta, Hymenoptera). *Zeischrift fur Zoologische, Systematische, Evolution Forschrung* **28:** 48–61.

Wagner GP, Altenberg L. 1996. Complex adaptations and the evolution of evolvability. *Evolution* **50:** 967–976.

Wagner GP, Booth G, Bagheri H. 1997. A population genetic theory of canalization. *Evolution* **51:** 329–347.

Wainwright PC. 2007. Functional versus morphological diversity in macroevolution. *Annual Review of Ecology Evolution and Systematics* **38:** 381–401.

Wainwright PC, Bellwood DR, Westneat MW, Grubich JR, Hoey AS. 2004. A functional morphospace for the skull of labrid fishes: patterns of diversity in a complex biomechanical system. *Biological Journal of the Linnean Society* **82:** 1–25.

Walker JA. 1997. Ecological morphology of lacustrine threespine stickleback *Gasterosteus aculeatus* L. (Gasterosteidae) body shape. *Biological Journal of the Linnean Society* **61:** 3–50.

Walker JA, Bell MA. 2000. Net evolutionary trajectories of body shape evolution within a microgeographic radiation of threespine sticklebacks (*Gasterosteus aculeatus*). *Journal of Zoology* **252:** 293–302.

Westneat MW. 1990. Feeding mechanics of teleost fishes (Labridae; Perciformes): A test of four-bar linkage models. *Journal of Morphology* **205:** 269–295.

Willacker JJ, Hippel FA, Wilton PR, Walton KM. 2010. Classification of threespine stickleback along the benthic–limnetic axis. *Biological Journal of the Linnean Society* **101:** 595–608.

Young NM, Hallgrimsson B. 2005. Serial homology and the evolution of mammalian limb covariation structure. *Evolution* **59:** 2691–2704.

Zelditch ML. 1988. Ontogenetic variation in patterns of developmental and functional integration in the laboratory rat. *Evolution* **42:** 28–81.

Zelditch ML, Wood AR, Bonett RM, Swiderski DL. 2008. Modularity of the rodent mandible: integrating bones, muscles, and teeth. *Evolution and Development* **10:** 756–768.

ARCHIVED DATA

Data deposited at Dryad: doi:10.5061/dryad.4b5c4 (Jamniczky *et al*., 2013).

SUPPORTING INFORMATION

Additional Supporting Information may be found in the online version of this article at the publisher's web-site:

Figure S1. Principal components analysis of shape variation in each of the four individual opercular bones: interopercle (A), opercle (B), preopercle (C), and subopercle (D). Percentages indicated on the principal component (PC) axes indicate percent of total variance explained by each PC. Ellipses represent 95% equal frequency ellipses for each population. BP, Bear Paw Lake; Bt, Boot Lake; RS, Rabbit Slough.